TOXICOLOGICAL SCIENCES **119(2)**, 359–368 (2011)
doi:10.1093/toxsci/kfq349
Advance Access publication December 1, 2010

Surface Derivatization State of Polystyrene Latex Nanoparticles Determines both Their Potency and Their Mechanism of Causing Human Platelet Aggregation *In Vitro*

Catherine McGuinnes,* Rodger Duffin,* Simon Brown,* Nicholas L. Mills,† Ian L. Megson,‡ William MacNee,* Shonna Johnston,* Sen Lin Lu,§ Lang Tran,¶ Rufia Li,‖ Xue Wang,‖ David E. Newby,† and Ken Donaldson*,¶,[1]

**Centre for inflammation Research, University of Edinburgh, Edinburgh, EH16 4TJ, UK; †Centre for Cardiovascular Sciences, University of Edinburgh, Edinburgh EH16 4TJ, UK; ‡Free Radical Research Facility, UHI Millennium Institute, Inverness, IV2 3BL, UK; §School of Environmental and Chemical Engineering, University of Shanghai, Shanghai, China; ¶Institute of Occupational Medicine, Edinburgh EH14 4AP, UK; and ‖Institute of Particle Science and Engineering, University of Leeds, Leeds LS2 9JT, UK*

[1]To whom correspondence should be addressed at Centre for inflammation Research, University of Edinburgh, 47 Little France Crescent, Edinburgh, Midlothian EH16 4TJ, UK. Fax: +44-131-242-6582. E-mail: ken.donaldson@ed.ac.uk.

Received September 2, 2010; accepted November 12, 2010

There is evidence that nanoparticles (NP) can enter the bloodstream following deposition in the lungs, where they may interact with platelets. Polystyrene latex nanoparticles (PLNP) of the same size but with different surface charge—unmodified (umPLNP), aminated (aPLNP), and carboxylated (cPLNP)—were used as model NP to study interactions with human blood and platelets. Both the cPLNP and the aPLNP caused platelet aggregation, whereas the umPLNP did not. Whereas cPLNP caused aggregation by classical upregulation of adhesion receptors, aPLNP did not upregulate adhesion receptors and appeared to act by perturbation of the platelet membrane, revealing anionic phospholipids. Neither oxidative stress generation by particles nor metal contamination was responsible for these effects, which were a result of differential surface derivatization. The study reveals that NP composed of insoluble low-toxicity material are significantly altered in their potency in causing platelet aggregation by altering the surface chemistry. The two surface modifications, aminated and carboxylated, that did cause aggregation did so by different mechanisms. The study highlights the fundamental role of surface chemistry on bioactivity of NP in a platelet activation model.

Key Words: **nanoparticles; platelets; aggregation; nanotoxicology.**

Epidemiological studies have clearly demonstrated that the level of air pollution particles, normally measured as particulate matter $(PM)_{10}$ or $PM_{2.5}$, is an important risk factor in lung disease (Abbey *et al.*, 1998; Dockery *et al.*, 1993; Goldberg *et al.*, 2000), and it is also well established that there is an association of increased levels of ambient particles with cardiovascular morbidity and mortality (Committee on the Medical Effects of Air Pollutants, 2006; Mills *et al.*, 2009).

It has been hypothesized that the most hazardous fraction of PM is the combustion-derived nanoparticles (CDNP; diameter < 100 nm) produced from combustion of fossil fuels by motor vehicles and power generators (Donaldson *et al.*, 2003, 2004). Chamber studies by our own group demonstrate that acute exposure to diesel soot, a key CDNP in urban air, causes endothelial dysfunction and fibrinolytic imbalance in healthy volunteers (Mills *et al.*, 2005) enhances thrombotic potential of peripheral blood, and enhances myocardial ischemia in exercising patients with coronary artery disease (Mills *et al.*, 2007). Chronic exposure to PM is also associated with development of coronary heart disease (Kunzli *et al.*, 2005) as demonstrated by an association between long-term exposure to $PM_{2.5}$ and carotid intima-media thickness in subjects living in different areas of Los Angeles.

By implication, manufactured NP have also come under suspicion because of their small size and large and potentially reactive surface area (Borm *et al.*, 2006; Oberdorster *et al.*, 2005). The potential mechanisms responsible for adverse effects of ultrafine/NP on the cardiovascular system are under investigation, and several have been proposed. Inhaled particles accumulating in the lungs may cause systemic inflammation and oxidative stress, which mediates endothelial dysfunction and atherosclerosis (Donaldson *et al.*, 2005; Le Brocq *et al.*, 2008). The systemic inflammation may also increase the propensity for thrombosis by activating platelets and coagulation factors such as fibrinogen (Donaldson *et al.*, 2001; Nadziejko *et al.*, 2002; Pekkanen *et al.*, 2000). In contrast to microsized particles, NP might escape macrophage phagocytosis (Renwick *et al.*, 2001) and translocate across the epithelial barrier, allowing direct interaction with endothelial cells and blood constituents (Geiser *et al.*, 2005). Although this has been demonstrated in a number of animal studies (Krieger

TABLE 1
Characteristics and Source of the PLNP Used in the Study

Description	Acronym	Size (nm)		Zeta potential (mV)	
		Buffer[a]	Plasma[b]	Buffer	Plasma
PLNP unmodified, Polysciences 08691-10	umPLNP	73.4 (1.7)	87.7 (2.7)	−25.7 (2.7)	−11.8 (0.3)
PLNP, carboxylated, fluorescent blue, Polysciences 19773-10	cPLNP	78.7 (1.8)	78.9 (1.5)	−30.1 (1.2)	−17.5 (0.7)
PLNP, aminated, fluorescent blue, Sigma L0780	aPLNP	63.3 (1.7)	75.3 (2.5)	−13.4[c] (0.3)	−15.7 (1.6)

[a]0.35% Plasma.
[b]50% Plasma.
[c]Zeta potential of aPLNP in saline with no plasma was +12.1 (1.0).

et al., 2002), reports from human studies with inhaled 99m Technetium-labeled NP and detection by γ camera imaging are more controversial (Mills *et al*., 2005a). In 1977, (Berry *et al*. 1977) observed that gold particles (30 nm), delivered to rat lungs by intratracheal instillation, crossed the alveolar capillary barrier and accumulated in platelets; the authors suggested that this might represent a transport mechanism for delivering the smallest air pollutant particles, such as tobacco smoke, to distant organs. They also concluded that it might predispose to platelet aggregation with formation of microthrombi and enhance the thrombotic consequences of atheromatous plaque rupture, should it occur. Enhancement of experimentally induced peripheral thrombosis and platelet activation also occurs following intratracheal instillation of 60 nm positively charged polystyrene particles (Nemmar *et al*., 2002a) and diesel exhaust particles to experimental animals (Nemmar *et al*., 2002b, 2003b). Radomski and Jurasz (2005) have demonstrated differences between carbon NP in their ability to activate platelets and enhance vascular thrombosis. Air pollution particles (Sun *et al*., 2005) and carbon nanotubes (Li *et al*., 2007) are known to enhance atherosclerosis in Apolipoprotein A knockout mice. Therefore, there is extensive potential for adverse atherothrombotic effects of NP.

The translocation of NP from the lung surface into the bloodstream has been proposed as one possible mechanism for adverse cardiovascular effects of ambient particles, and manufactured NP now pose the same potential risks (Donaldson and Stone, 2007). Limited studies have shown that NP in the blood may activate platelets causing increased adhesion and aggregation (Nemmar *et al*., 2002a; Radomski and Jurasz, 2005), so increasing the potential for thrombosis. Activated platelets also release potent inflammatory and mitogenic substances into the local microenvironment, thereby altering chemotactic, adhesive, and proteolytic properties of endothelial cells contributing to inflammation and atherogenesis (Gawaz, 2004).

There is a need to understand the effects of particle characteristics, such as size and chemical composition on the various endpoints of particle toxicity. In this study, we kept the nanoparticle size constant at about 50 nm and varied surface chemistry and examined the effect this had on platelets *in vitro*. In doing so, we tested the hypothesis that different surface modifications of polystyrene latex nanoparticles (PLNP) of the same size would modify their ability to activate platelets. This hypothesis therefore seeks to explore whether NP surface chemistry affects a potentially key biological activity when nanoparticle size is kept constant and in the absence of soluble particle products that might also affect the target cell.

MATERIALS AND METHODS

Polystyrene Latex Nanoparticles

Unmodified, aminated, and carboxylated polystyrene latex nanobeads were selected for consistency of size and composition (Table 1). In order to examine bead morphology, the particles were dried on aluminum stubs, coated with gold, and examined using scanning electron microscopy.

Analysis of Metal Content of the Particles

The samples were prepared for analysis of their metal content using a modification of Occupational Safety and Health Administration ID121 (OSHA, 1991) and analyzed by inductively coupled plasma/atomic emission spectrometry after desorption in deionized water (10 ml). The limit of detection for metals by this method is 0.1 μg/g or 0.01 μg/ml.

Electron Paramagnetic Resonance

Nanoparticles were made up to 250 μg/ml in Hanks balanced salt solution (HBSS) (Sigma, Dorset, UK) and sonicated for 5 min. HBSS and 1mM pyrogallol (Sigma), a known superoxide generator, served as negative and positive controls, respectively. Ten milliliters of Tempone H (Alexis, San Diego, CA) (10^{-1}M made up in 10^{-2}M EDTA solution), a spin trap shown to quantify peroxynitrite and superoxide radical formation (32; Dikalov *et al*., 1997), was added to the controls and nanoparticle suspensions incubating at 37°C. After 60 min, samples were vortexed and a 50-ml aliquot drawn into a glass capillary tube, which was then sealed at one end. The capillary was inserted into an electron paramagnetic resonance (EPR) spectrometer (MS200 Miniscope; Magnettec, Germany) and the characteristic three-line signal generated through formation of the corresponding spin adduct of Tempone H (4-oxo-tempo) recorded at 60 min. The settings of the EPR were as follows:

magnetic field, 3355 G; sweep width, 55 G; scan time, 30 s; number of passes, 1; modulation amplitude, 1500 mG; receiver gain, 1E1; phase, 180; microwave frequency, 9.30–9.55 GHz.

Blood Collection

The following blood collection technique was used in order to minimize platelet activation during blood collection: a light tourniquet was used or none at all and a 19 G needle was utilized. Smooth flow was ensured and the first 2 ml were discarded. Blood was collected from normal human volunteers aged 25–60 years with no reported medication into P-Pack tubes (Sarstedt, Leicester, UK) and mixed thoroughly by repeated gentle inversion.

Determination of bead association. Peripheral blood was drawn as above into a P-Pack tube. Fifty nanometers carboxylated PLNP (cPLNP) (Polysciences Inc., Eppelheim, Germany) were sonicated for 10 min and 10 μl added to 1 ml whole blood giving a final concentration of 260 μg/ml and gently mixed (5 s). One hundred microliters of the blood bead mixture was added immediately to 100 μl of antibody cocktail containing CD14-Phycoerythrin (CD14 PE) (Biosource: Invitrogen, Paisley, UK) and CD42a-Fluorescein isothyocyanate (FITC) (BD Pharmingen, San Diego) (1:20) in modified Hepes-Tyrode's buffer. Samples were incubated in the dark for a period of 20 min prior to addition of 1× fluorescence activated cell sorter (FACS) Lyse (1500 μl; BD Pharmingen) to fix the cells and lyse the erythrocytes. After a further 15-min incubation period under the same conditions, samples were analyzed using the BD FACSVantage SE with the DiVa option. A control sample of blood containing 10 μl/ml 0.9% NaCl was treated and analyzed in the same manner.

The monocyte population was identified on the basis of its characteristic light scatter properties in linear mode on the forward scatter (FSC) × side scatter (SSC) parameters. A marker identifying CD14-PE–expressing cells was then used to confirm the position of the CD14-positive monocyte population within the gate. An isotype FITC (BD Pharmingen) control was used to set the quadrant gate for nonspecific FITC fluorescence. Gates were set around the following populations: CD14 positive, CD42a positive, CD14 positive/CD42a positive, and CD14 negative/CD42a negative. The treated samples were analyzed by a ultraviolet (UV) laser, and the resulting blue light emission at 325 nm showed association with the fluorescent 50 nm cPLNP. As a control, 50 nm cPLNP were run independently to show that they fall out with the gate. The four gated populations were sorted into 1 ml of medium. A further 5 ml of phosphate-buffered saline (Sigma) was added to each tube, and the samples were centrifuged at 1200 revolutions per minute (rpm) for 10 min. The cells were resuspended in 50 μl of medium, which was then transferred to a slide and allowed to dry overnight in the dark prior to being mounted in Mowiol and viewed by confocal microscopy Zeiss laser scanning microscope Confocal Microscope with 488 nm laser with Hg lamp and UV Filter set for bead emission.

Effect of NP on whole blood. Two hundred and sixty micrograms per milliliter 50 nm PLNP (unmodified [Polysciences Inc.], aminated [Sigma], and carboxylated [Polysciences Inc.]) were added to whole blood and mixed gently (5 s). Equal volumes of blood/bead mixture and antibody cocktail of CD42a-FITC, CD14-PE, and CD16 PE-Cy5 (BD Pharmingen) (1:20) in modified Hepes-Tyrode buffer were incubated in the dark at room temperature for 20 min prior to addition of 500 μl of 1× FACS Lyse to fix the cells and lyse the erythrocytes. A sample of blood containing 10 μl/ml 0.9% NaCl was treated and analyzed in the same manner.

The monocyte population was identified as above on the basis of its characteristic light scatter properties in linear mode on the FSC × SSC parameters. A marker identifying CD14-PE–expressing cells was then used to confirm the position of the monocyte population and select CD14-positive cells within the gate. An isotype FITC (BD Pharmingen) control was used to set the quadrant gate for nonspecific FITC fluorescence. Two thousand five hundred CD14-positive events were collected using the BD FACS Caliber allowing for analysis of the following populations: CD14 positive/Cd42a negative, CD14 positive/Cd42a positive, and CD42a positive. The neutrophil population was identified as above on the basis of its characteristic light scatter properties in linear mode on the FSC × SSC parameters. A marker identifying CD16-PE-Cy5–expressing cells was then used to confirm the position of neutrophil population and select CD16-positive cells within the gate. An isotype FITC (BD Pharmingen) control was used to set the quadrant gate for nonspecific FITC fluorescence. Seven thousand five hundred CD16-positive events were collected using the BD FACS Caliber allowing for analysis of the following populations: CD16 positive/Cd42a negative and CD16 positive/Cd42a positive.

Effect of soluble metals on whole blood. To check that there was no role for soluble metals, we prepared an aqueous extract from the three particle types by suspending in distilled water and agitating for 24 h at which point the particles were spun out by high-speed centrifugation. This aqueous extract was used to treat whole blood at the concentration that was effective in causing platelet aggregation and stained as above.

Effect of NP on isolated platelets. Isolated platelets were prepared by centrifuging (5 ml; 10 min at 2500 rpm) platelet-rich plasma with prostacyclin (300nM) (Sigma) to prevent platelet aggregation (Sigma, Poole, UK). The platelet pellet was resuspended in 5 ml of modified Hepes-Tyrode buffer and left to recover (45 min). Unmodified PLNP (umPLNP), aminated PLNP (aPLNP), and cPLNP were added at 260 μg/ml and the mixture gently mixed (5 s). An aliquot (5 ml) of the platelet/bead mixture was added to 35 μl of antibody cocktail containing CD62-P and the platelet-binding antibody PAC-1 (1:20) (BD Pharmingen) in modified Hepes-Tyrode buffer. Samples were incubated in the dark (20 min) prior to addition of 800 μl of 1% paraformaldehyde in PBS to fix the cells. Five microliters of 0.9% NaCl (negative control) and 10μM thrombin receptor activator peptide (TRAP-positive control) (Sigma) were treated and analyzed in the same manner. Seven thousand five hundred platelet events were collected for each sample. A control isotype PE was used to set the quadrant gate for nonspecific PE fluorescence, and an RGDS peptide sequence (Sigma), which inhibits PAC-1 binding, was used to set the quadrant gate for nonspecific FITC fluorescence.

Effect of NP on Annexin V binding. Isolated platelets were prepared as above. umPLNP, aPLNP, and cPLNP were added at 260 μg/ml and equal volumes of the platelet/bead mixture and Annexin V-PE (1:20) (BD Pharmingen) in Modified Hepes-Tyrode's buffer with 6mM $CaCl_2$. Samples were incubated in the dark for 20 min prior to addition of a further 800 μl of the above buffer. Seven thousand five hundred platelet events were collected using flow cytometry (BD FACS Caliber).

Ability of NP to cause erythrocyte hemolysis. An erythrocyte hemolysis assay was conducted in order to determine the effect of different PLNP on membrane surface integrity. Briefly, erythrocytes were obtained from fresh human venous blood following removal of plasma and buffy-coat layer and subsequent washes. The washed erythrocytes were incubated with 0.9% NaCl (negative control), umPLNP, aPLNP, cPLNP, DQ12 standard quartz (known to cause erythrocyte hemolysis), and Triton X (positive control) (Sigma) for a period of 20 min in the dark at room temperature. The subsequent percentage of hemolysis was determined by measuring the absorbance at 550 nm.

Statistical Analysis

All data were tested for statistical significance using ANOVA with a Tukey post-test in Instat (Graph Pad Software).

RESULTS

Particle Size

As is shown in Figure 1, in appearance, the particles were spherical and had a diameter that was consistent with the target 50-nm size range described by the suppliers. Table 1 shows the size of the particles determined by dynamic light scatter in buffer containing 0.35% plasma to mimic the levels found in the isolated platelet assay and in 50% plasma to more closely mimic the conditions in the whole-blood assay, Although

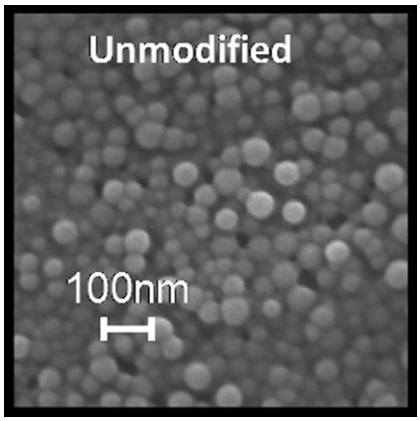

FIG. 1. Scanning electronic microscope image of the unmodified beads; all the bead samples were identical in appearance and size to the unmodified shown here.

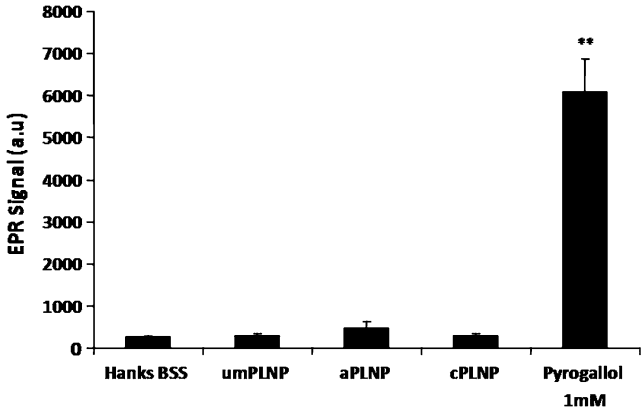

FIG. 2. Free-radical generation by polystyrene latex nanobeads with various surface modifications as measured by EPR with HBSS and 1mM pyrogallol as negative and positive controls, respectively. Tempone H (1mM) was used as the spin trap (***$p < 0.001$). Mean ± SEM values shown, $n = 3$.

whole blood has 100% plasma, this level caused interference in the dynamic light scattering and the zeta potential studies, and so 50% was used. There was no significant change in particle size on incubation in plasma showing no particle-aggregating effect of plasma.

Zeta Potential

As shown in Table 1, all the particles had a negative zeta potential in buffer (0.35% plasma) and in 50% plasma. For unmodified beads and carboxylated beads, 50% plasma caused a marked decrease in the zeta potential. In the case of the aminated beads, increasing the plasma concentration from 0.35 to 50% had little effect on zeta potential, but we note that in protein-free conditions, the aminated beads had a positive zeta potential of 12.1 mV.

Metal Analysis

None of the particles had significant levels of soluble metals, none exceeding 4.5 μg/g being the iron level in carboxylated beads (Table 2). There was minor variation in the metal content of the beads, where Zn was highest in the aminated beads (0.38 μg/g in unmodified beads, 1.38 μg/g in aminated beads, and 0.18 μg/g in carboxylated beads).

EPR Analysis of Particles

TABLE 2
Soluble Metal Associated with the Three Particle Types

	Metal concentration (μg/g)									
Surface	Cd	Co	Cr	Cu	Fe	Mn	Ni	Ti	V	Zn
Unmodified	< 0.01	< 0.01	0.02	0.23	0.37	0.02	0.16	0.03	< 0.01	0.32
Aminated	< 0.01	0.04	0.01	0.46	1.64	0.03	0.04	0.32	< 0.01	1.38
Carboxylated	< 0.01	0.04	< 0.01	0.16	4.46	0.19	< 0.01	0.01	< 0.01	0.18

In order to determine if any differences between the particles that might be seen in platelet activation is because of differences in the PLNP to generate oxidative stress, we determined the generation of oxygen-centered free radicals by the three bead samples using EPR. Free radicals were detected using a Tempone H spin trap that captures most species of free radicals. None of the PLNP caused any detectable free-radical generation; in contrast, pyrogallol a recognized spontaneous superoxide anion generator produced a large free-radical signal (Fig. 2).

Determination of Association of Beads with Platelets by Flow Cytometry and Confocal Microscopy

Collection of events within the monocyte gate was determined using FSC and SSC. Using dual-staining for CD42a and CD14, monocyte-platelet aggregates were observed, but low numbers of free monocytes and platelet aggregates (which are CD42-positive and CD14-negative events) were noted in the monocyte gate. These CD42-positive events were platelet aggregates because single platelets, because of their small size, do not appear in the monocyte gate. Incubation of cPLNP with whole blood produced a striking increase in the CD42-positive events collected within the monocyte gate, i.e., increased platelet aggregates, with a measurable decrease in platelet-monocyte complexes. UV-fluorescent cPLNP alone run through the flow cytometer and do not fall within the gated population and are therefore not detected (data not shown). In whole blood incubated with cPLNP, analysis of UV-positive events within the monocyte gate indicating cPLNP binding revealed that 100% of the platelet-platelet aggregates (highly expressing CD42a positive/CD14 negative) had UV-fluorescent cPLNP associated with them compared with only 47% of platelet-monocyte complexes (CD14 positive/CD42a positive). No free monocytes (CD14 positive/CD42a negative) were shown, indicating

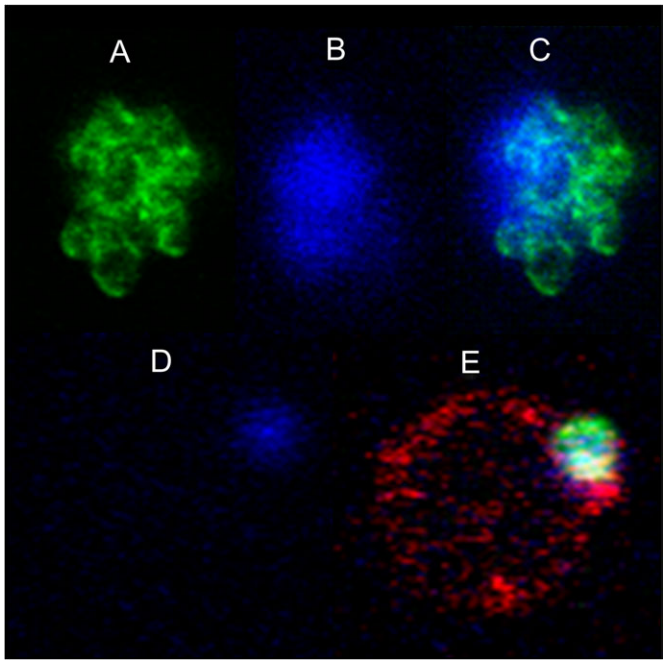

FIG. 3. Upper panel shows confocal microscopy images (original magnification ×100) showing platelet-platelet aggregates stained with CD42a-FITC (A) latex beads by UV illumination (B) and colocalization of beads and platelet aggregates using both forms of illumination (C). Lower panel (E) shows confocal microscopy images (original magnification ×100) showing a monocyte-platelet aggregate stained with CD14-PE (red color monocyte) and CD42a-FITC (green color platelets) overlain with the blue UV-illuminated NP (shown alone in D) to demonstrate a nanoparticle-platelet-monocyte complex.

that cPLNP are associated only with platelet populations in platelet-platelet or monocyte-platelet aggregates.

Populations of interest were collected and subjected to visualization using confocal microscopy. Under UV light, no fluorescent cPLNP were observed within the CD14-positive/CD42a-negative population, indicating that cPLNP do not associate with monocytes alone. The highly expressing CD42a-positive/CD14-negative population contained platelet aggregates, which under UV light demonstrated an association with the UV-fluorescent cPLNP (Figs. 3A–C). With respect to

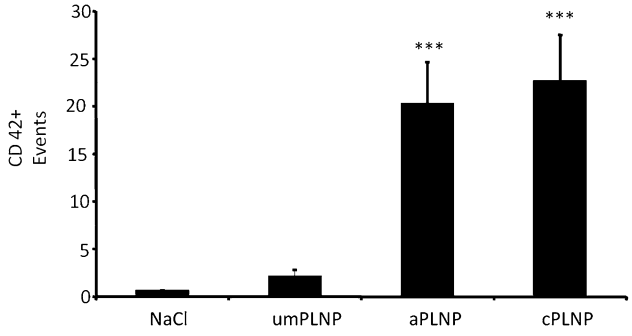

FIG. 4. Platelet aggregates formed in whole blood by treatment with aPLNP and cPLNP but not umPLNP. Bars represent mean + SEM of $n = 3$ separate experiments.

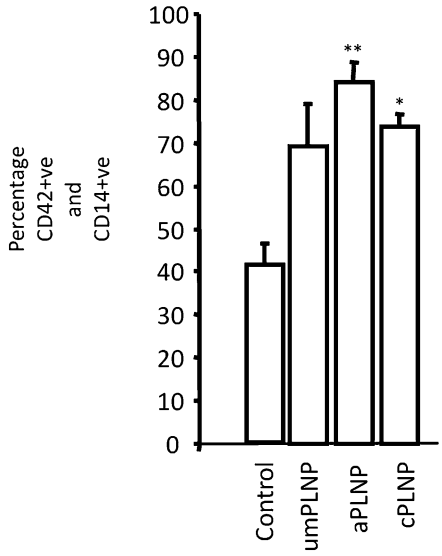

FIG. 5. Platelet-monocyte aggregates following treatment of whole blood with the various PLNP. Asterisks denote significant difference from control—there was no difference between the levels of aggregates seen between the three PLNP.

the CD14-positive/CD42a-positive cell population, platelets were observed attached to monocytes; furthermore, UV illumination showed cPLNP in association with the platelets complexed to monocytes (Figs. 3D–E).

Effect of NP and aqueous extracts of NP on Whole Blood

Both aPLNP and cPLNP caused a significant increase in platelet-platelet aggregates compared with the saline control and the umPLNP, which had no significant effect on aggregation (Fig. 4). No significant differences in polymorphonuclear neutrophilic leucocyte-platelet aggregates were observed between any PLNP and the saline control (data not shown). Platelet-monocyte aggregation, assessed as percentage of CD14-positive events that were also CD42b positive, is shown in Figure 5. Although aPLNP and cPLNP treatment of blood caused significantly more platelet-monocyte aggregates than were seen in the control blood, there was no significant difference between the three PLNP types in terms of their

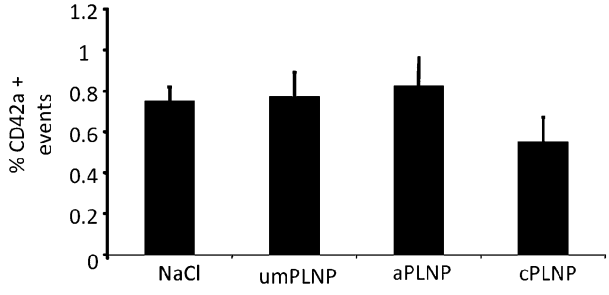

FIG. 6. Effect of Aqueous extract (AE) of beads on aggregate formation; note the vertical scale showing no significant platelet aggregation effects. Bars represent mean + SEM of $n = 3$ separate experiments.

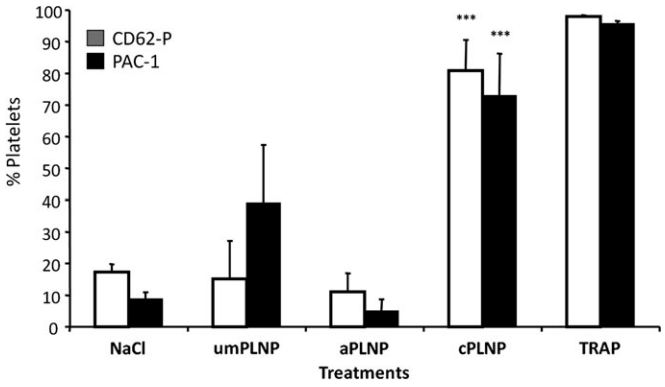

FIG. 7. Expression of CD62-P (P-selectin) and PAC-1 in platelets following treatment of whole blood with the various PLNP plus positive control TRAP; significant ($p < 0.001$) increase over NaCl seen only with cPLNP and TRAP. Bars represent mean + SEM of $n = 3$ separate experiments.

potency in inducing platelet-monocyte aggregates. Aqueous extracts prepared for all three particle types had no effect on platelet-platelet aggregates (Fig. 6).

Whole blood treated with umPLNP and aPLNP did not show any increase in CD62P or PAC-1 expression compared with the saline control. Treatment with cPLNP, however, resulted in significant expression of CD62P and PAC-1 on par with the potent platelet activator TRAP (Fig. 7).

Effect of NP on Isolated Platelets

CD62P and PAC-1. Isolated platelets treated with umPLNP and aPLNP were not significantly different in CD62P or PAC-1 expression to the saline control. Treatment with cPLNP, however, resulted in significant expression of CD62P and PAC-1 on par with the potent platelet activator TRAP (Fig. 8).

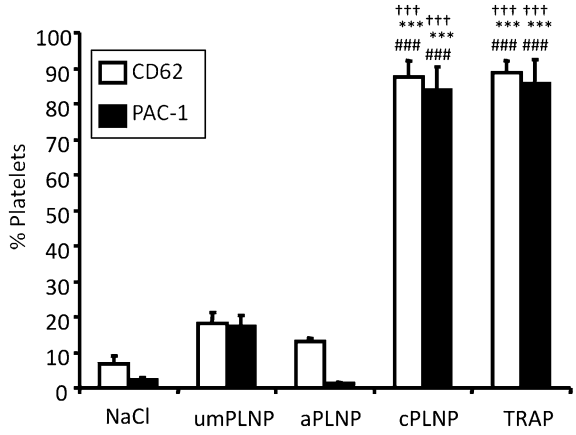

FIG. 8. Expression of CD62-P (P-selectin) and PAC-1 following treatment with the various PLNP and the positive control TRAP (platelet agonist). cPLNP and TRAP caused significant binding of CD62-P and PAC-1 compared with saline control (***$p < 0.001$), umPLNP (†††*$p < 0.001$), and aPLNP (###$p < 0.001$). Mean ± SEM values shown, $n = 3$.

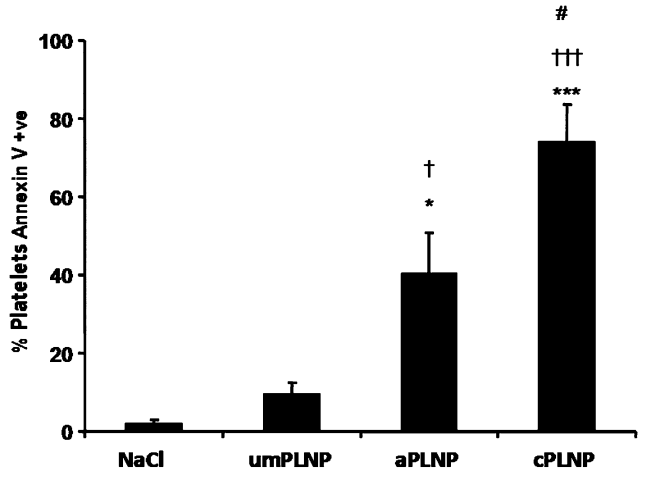

FIG. 9. Percentage of cells with phosphatidylserine on the external face of the plasma membrane as measured by Annexin V binding in response to 260 μg/ml of umPLNP, aPLNP, and cPLNP. aPLNP and cPLNP showed a significant difference to control (*$p < 0.0.01$ and ***$p < 0.001$) and umPLNP († $p < 0.01$ and †††$p < 0.001$), and cPLNP differed significantly to the aPLNP (#$p < 0.01$). Mean ± SEM values shown, $n = 4$.

Annexin V binding. Both aPLNP and cPLNP treatment of platelets induced significant binding of Annexin V compared with saline control and umPLNP, indicating relocation of phosphatidylserine to the outer plasma membrane (Fig. 9). cPLNP resulted in significantly greater levels of Annexin V binding than aPLNP.

Ability of NP to cause erythrocyte hemolysis. The erythrocyte membrane was used as a model membrane to investigate the above finding that aPLNP could directly disrupt the platelet membrane such that phosphatidylserine was revealed on the

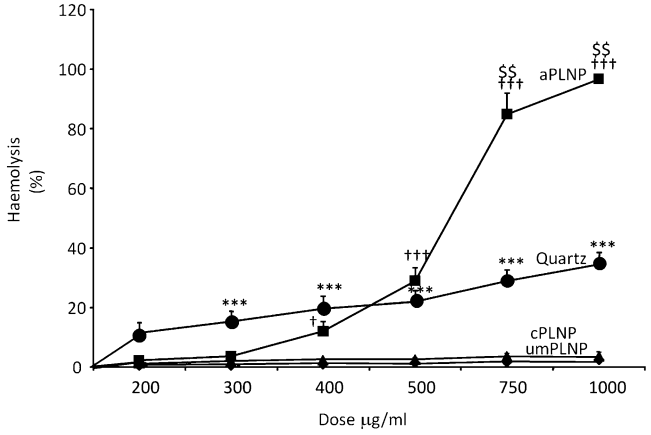

FIG. 10. Red blood cell (RBC) hemolysis in response to increasing doses of umPLNP, aPLNP, cPLNP, and DQ12 quartz. umPLNP and cPLNP caused no RBC hemolysis. Quartz caused significant hemolysis at all doses (***$p < 0.001$). aPLNP resulted in highly significant hemolysis at 500 μg/ml (†††$p < 0.001$), and by 750 μg/ml, this was significantly different to quartz ($$$$p < 0.001$). Mean ± SEM values shown, $n = 4$.

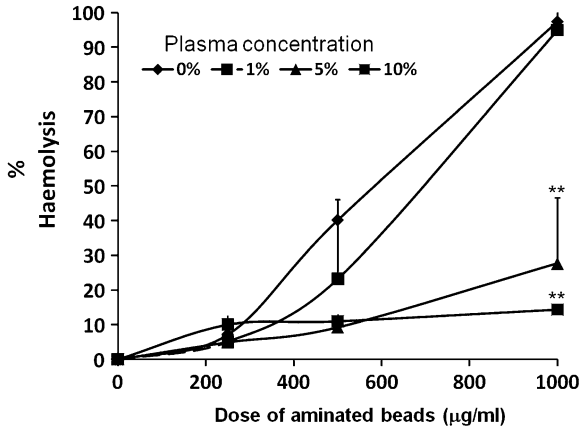

FIG. 11. Effect of 1, 5, and 10% plasma on hemolysis caused by aPLNP. There was no significant effect of 1% plasma, but 5 and 10% plasma cause significant inhibition of hemolysis **, $p < 0.01$ compared with 0% plasma. Mean ± SEM values shown, $n = 3$.

outside face of the plasma membrane. Damaging effects are detected in this assay where hemoglobin leaks from membranes damaged by interaction with the particles. aPLNP caused a highly significant erythrocyte hemolysis at 500 μg/ml with the observed erythrocyte hemolysis being significantly increased above that of quartz at 750 μg/ml (Fig. 10). Neither umPLNP nor cPLNP induced any significant erythrocyte membrane lysis. All concentrations of the quartz particles tested produced significant erythrocyte hemolysis in a dose-dependent manner. We also analyzed the effect of plasma on hemolysis and show that in the presence of even moderate (5%) plasma concentrations, hemolysis was abolished (Fig. 11).

DISCUSSION

There are a number of studies suggesting that NP that deposit in the lungs enter the circulation (Kreyling *et al*., 2002; Nemmar *et al*., 2004; Semmler *et al*., 2004) where they could interact with elements of the blood and the vascular wall, so explaining proatherothrombotic effects seen in a number of models (Hamoir *et al*., 2003; Mills *et al*., 2009; Nemmar *et al*. 2003a,b; Radomski and Jurasz, 2005). To further investigate the role of NP surface modification in such direct cardiovascular effects of NP, we utilized umPLNP, aPLNP, and cPLNP, respectively. There were both quantitative and qualitative differences in the mechanism of platelet activation caused by the PLNP, depending on their surface modification.

When comparisons were made between umPLNP, aPLNP (positively charged), and cPLNP (negatively charged), all were found to promote formation of platelet-monocyte aggregates to the same extent with no significant difference between the treatment groups. However, differences were noted in platelet-platelet aggregation between beads with different surface modifications, namely, that cPLNP and aPLNP were aggregation inducers, whereas umPLNP were not. An effect of nanoparticle surface modification in thrombosis has been previously described in a model of thrombosis in hamsters (Nemmar *et al*., 2002a). Iv instillation of umPLNP or negatively charged cPLNP had no significant effect on the experimental thrombus size compared with saline. However, iv instillation of positively charged aPLNP significantly enhanced thrombus generation. In parallel studies, these investigators incubated platelets with the different types of PLNP and found platelet-aggregating potency in the rank: unmodified < carboxylated < aminated, in keeping with the order of potency in causing thrombosis. Our findings are in general agreement with these previous findings, although we did not find any difference between cPLNP and aPLNP in ability to cause platelet aggregation. This could be a result of using flow cytometry rather than the platelet aggregometry approach used by the Nemmar study or difference between rodent and human platelet responses to NP.

Platelet-monocyte binding is considered to be an early marker of platelet activation. Our study found no difference between the three particle types in inducing platelet-monocyte aggregates. These findings raise questions relating to whether platelet-monocyte binding successfully predicts platelet aggregation caused by direct interaction with particles. Following injection into the blood of hamsters, Nemmar *et al*. (2003a) found enhanced thrombogenesis only with aPLNP. This suggests that there is nonspecificity in the monocyte-platelet-aggregating potential of PLNP but that platelet-platelet aggregates are more predictive at least of ability to cause enhanced thrombosis in the hamster model.

In the present study, we carried out comparison of CD62P expression and PAC-1 binding induced by cPLNP and aPLNP in order to understand the mechanism of the increased binding these two particles induced. In both buffer with 0.35% plasma and whole blood (100% plasma), only cPLNP promoted a marked upregulation, whereas the aPLNP did not. The control platelet agonist TRAP was a potent activator of CD62P expression and PAC-1 binding. Thus, a classical platelet activation phenotype was induced by cPLNP and was very likely the mechanism for promotion of platelet-platelet aggregation seen with the cPLNP. The finding that the aPLNP caused platelet-platelet aggregates to the same extent as cPLNP but did not do so by the classical adhesion pathway of increased CD62P and PAC-1 expression is a paradox.

During normal platelet hemostatic function, following direct interaction with damaged vessel walls, there is platelet activation, aggregation, and formation of a hemostatic plug. The exposed determinants on the plug serve as binding sites for prothrombinase complex (including prothrombin and coagulation factors Xa and Va) assembly, which markedly enhances the generation of thrombin, a key factor in hemostasis. The activated platelet membrane has increased expression of anionic phospholipids that promote coagulant activity and can be detected by the binding of the protein Annexin V (Hanshaw and Smith, 2005). When this assay was carried out on platelets

treated with the various PLNP, both cPLNP and aPLNP caused a significant increase in Annexin V binding. This demonstrated that, although aPLNP-treated platelets were not classically activated for PAC-1 and CD62-P upregulation, they did have increased anionic phospholipid exposure on their surface.

Nanoparticle aggregation is considered to be important in determining toxicity, and so it was necessary to investigate the size of the three NP in the different media used for the assay in order to be able to compare the effects of the PLNP between assays. There was good dispersion of the PLNP in all the conditions used with sizes consistent with singlet NP, consistent with the high zeta potentials seen in the two different media containing 0.35 or 50% plasma (Meissner *et al.*, 2009).

Erythrocytes and platelets carry a net negative charge in view of the ionized sialic acid groups on the surface. We hypothesized that greater interaction between the erythrocyte membrane and the positively charged aPLNP surface underlay the increased membrane perturbation. We further hypothesized that the same underlying mechanism governed the interaction between the platelet membrane and the negatively charged cPLNP surface and that this lead to sufficient perturbation to cause increased phosphatidylserine on the external membrane. umPLNP and cPLNP caused no significant hemolysis, but aPLNP were highly potent, as potent as quartz, a highly hemolytic particle. However, in relating these data to the events in whole blood, we noted that the dramatic effect of aPLNP on hemolysis occurred in protein-free conditions, whereas the platelet aggregation assay took place in whole blood. Plasma effectively inhibited hemolysis at 5% but not 1%, suggesting that the hemolytic type of particle membrane interaction could not have occurred between aPLNP and platelet membranes in whole blood, where plasma is 100%. The relationship between plasma concentration, zeta potential, and hemolysis is, however, complex because we found that 0.35% plasma reversed the zeta potential of aminated beads from +12.1 to −13.4 mV, but three times this concentration—1% plasma—failed to affect hemolysis. Therefore, whereas hemolysis is driven by effects other than simple surface charge, it is also clear that platelet aggregation driven by the simple interaction between a positive aPLNP surface and a negatively charged platelet surface is unlikely. However, the charges on a nanoparticle in a mixed protein solution are complex, and previous studies have already shown that aminated beads take up a different profile of proteins and lipoproteins from those of PLNP with different surface and direction of charge (Lundqvist *et al.*, 2008). Therefore, although not investigated here, the type of protein on the surface of the NP might also be important in activating platelet they come into contact with, and this warrants further investigation. Whatever the cause, aPLNP-exposed platelets show induction of anionic phospholipids in the external platelet membrane, which may contribute to platelet aggregation by attracting unaltered, normal negatively charged membrane areas of adjacent platelets. By contrast, carboxylated beads likely cause expression of phosphatidylserine on their surface as the final event in the classical platelet activation pathway following conformational change and activation of GP11a/111b and surface expression of P-selectin.

Oxidative stress has been advanced as an explanation for the adverse actions of NP at the cellular level (Donaldson and Stone, 2007), and so we tested the three PLNP for the ability to generate free radicals using EPR. All the PLNP generated a very low EPR signal, and there was no difference between them. Oxidative stress, via particle-derived free radicals, is unlikely to be the explanation for the extra activity of the aPLNP. In addition, the metal concentration of the different samples was at a very low level in any of the PLNP. To check that there was no role for soluble metals, we prepared an aqueous extract from the three particle types at the concentration that was effective in causing platelet aggregation. These were tested for ability to cause platelet aggregation, and no activity was found. Therefore, different levels of soluble metals cannot explain the differences between PLNP types in causing platelet aggregation.

In summary, we used polystyrene latex nanobeads of the same size but with different surface chemistry and charge as a model NP to study the role of the surface in interactions with human platelets. We showed that NP in whole blood associated with platelets. We demonstrated that surface properties were important in causing platelet aggregation with the cPLNP and the aPLNP causing platelet aggregation, whereas the umPLNP did not. However, there were different mechanisms involved with the two aggregation-inducing PLNP with only cPLNP causing classical upregulation of adhesion receptors. By contrast, aPLNP appear to act via an unexplained mechanism that results in the display of anionic phospholipids on the external face of the platelet plasma membrane. Neither oxidative stress nor metal or any other soluble contamination could explain the ability of cPLNP and aPLNP to cause platelet aggregation. In the case of aPLNP, an unusual protein adsorption pattern might lead to membrane perturbation–mediated aggregation. The mechanism of cPLNP-mediated platelet aggregation remains obscure.

There is insufficient toxicokinetic data to predict the fraction of inhaled/deposited NP that become blood borne for specific types of NP, although the evidence is that this is a small fraction of the inhaled/deposited dose (Kreyling *et al.*, 2007). However, it is certain that the doses used in our experiments were significantly higher than would be expected to become blood borne, at least following inhalation. However, the aim here was to determine the potential of NP in the blood to have effects and to investigate the role of particle surface in any effects. The future accumulation of data on nanoparticle dosimetry in the blood following inhalation will allow better interpretation of such data as to whether effects may be seen at plausible exposures. Nevertheless, the results of this study indicate that particle surface chemistry is a vital consideration in establishing the extent to which NP impact on a significant cellular response, namely, platelet activation and on the

mechanism. This has significance for nanotoxicology testing for cardiovascular effects because, for the same size and composition of NP, surface modification affects the potency. In addition, where two differently surface-modified NP had similar platelet-activating potency, the underlying mechanism for the activation was different. This makes generalizations regarding the potential potency of NP comprised of the same materials impossible and makes thorough characterization of the surface charge and chemistry of NP surfaces a necessity.

FUNDING

European Union FP6 program in the Particle Risk project.

REFERENCES

Abbey, D. E., Burchette, R. J., Knutsen, S. F., McDonnell, W. F., Lebowitz, M. D., and Enright, P. L. (1998). Long-term particulate and other air pollutants and lung function in nonsmokers. *Am. J. Respir. Crit. Care Med.* **158,** 289–298.

Berry, J. P., Arnoux, B., Stanislas, G., Galle, P., and Chretien, J. (1977). A microanalytic study of particles transport across the alveoli: role of blood platelets. *Biomedicine* **27,** 354–357.

Borm, P. J., Robbins, D., Haubold, S., Kuhlbusch, T., Fissan, H., Donaldson, K., Schins, R. P., Stone, V., Kreyling, W., Lademann, J., *et al.* (2006). The potential risks of nanomaterials: a review carried out for ECETOC. *Part Fibre Toxicol.* **3,** 11.

Committee on the Medical Effects of Air Pollutants. (2006). *Cardiovascular Disease and Air Pollution*. Department of Health, London.

Dikalov, S., Skatchkov, M., and Bassenge, E. (1997). Quantification of peroxynitrite, superoxide, and peroxyl radicals by a new spin trap hydroxylamine 1-hydroxy-2,2,6,6-tetramethyl-4-oxo-piperidine. *Biochem. Biophys. Res. Commun.* **230,** 54–57.

Dockery, D. W., Pope, C. A., Xu, X. P., Spengler, J. D., Ware, J. H., Fay, M. E., Ferris, B. G., and Speizer, F. E. (1993). An association between air-pollution and mortality in 6 united-states cities. *N. Engl. J. Med.* **329,** 1753–1759.

Donaldson, K., Jimenez, L. A., Rahman, I., Faux, S. P., MacNee, W., Gilmour, P. S., Borm, P. J., Schins, R. P. F., Shi, T., and Stone, V. (2004). Respiratory health effects of ambient air pollution particles: role of reactive species. In *Oxygen/Nitrogen Radicals: Lung Injury and Disease Vol 187 in Lung Biology in Health and Disease Exec Ed Lenfant C* (V. Vallyathan, X. Shi, and V. Castranova, Eds.), pp. 257–288. Marcel Dekker, New York, NY.

Donaldson, K., Mills, N., MacNee, W., Robinson, S., and Newby, D. (2005). Role of inflammation in cardiopulmonary health effects of PM. *Toxicol. Appl. Pharmacol.* **207**(Suppl. 2), 483–488.

Donaldson, K., and Stone, V. (2007). Toxicological properties of nanoparticles and nanotubes. In *Issues in Environmental Science and Technology, Nanotechnology* (R. Harrison and R. Hester, Eds.), Vol. 24, pp. 81–96.

Donaldson, K., Stone, V., Borm, P. J., Jimenez, L. A., Gilmour, P. S., Schins, R. P., Knaapen, A. M., Rahman, I., Faux, S. P., Brown, D. M., *et al.* (2003). Oxidative stress and calcium signaling in the adverse effects of environmental particles (PM10). *Free Radic. Biol. Med.* **34,** 1369–1382.

Donaldson, K., Stone, V., Seaton, A., and MacNee, W. (2001). Ambient particle inhalation and the cardiovascular system: potential mechanisms. *Environ. Health Perspect.* **109**(Suppl. 4), 523–527.

Gawaz, M. (2004). Role of platelets in coronary thrombosis and reperfusion of ischemic myocardium. *Cardiovasc. Res.* **61,** 498–511.

Geiser, M., Rothen-Rutlshauser, B., Kapp, N., Schurch, S., Kreyling, W., Schulz, H., Semmler, M., Im, H., V, Heyder, J., *et al.* (2005). Ultrafine particles cross cellular membranes by non-phagocytic mechanisms in lungs and in cultured cells. *Environ. Health Perspect.* **113,** 1555–1560.

Goldberg, M. S., Bailar, J. C., III., Burnett, R. T., Brook, J. R., Tamblyn, R., Bonvalot, Y., Ernst, P., Flegel, K. M., Singh, R. K., and Valois, M. F. (2000). Identifying subgroups of the general population that may be susceptible to short-term increases in particulate air pollution: a time-series study in Montreal, Quebec. *Res. Rep. Health Eff. Inst.* **97,** 7–113.

Hamoir, J., Nemmar, A., Halloy, D., Wirth, D., Vincke, G., Vanderplasschen, A., Nemery, B., and Gustin, P. (2003). Effect of polystyrene particles on lung microvascular permeability in isolated perfused rabbit lungs: role of size and surface properties. *Toxicol. Appl. Pharmacol.* **190,** 278–285.

Hanshaw, R. G., and Smith, B. D. (2005). New reagents for phosphatidylserine recognition and detection of apoptosis. *Bioorg. Med. Chem.* **13,** 5035–5042.

Kreyling, W. G., Moller, W., Semmler-Behnke, M., and Oberdorster, G. (2007). Particle dosimetry: deposition and clearance from the respiratory tract and translocation to extra-pulmonary sites. In *Particle Toxicology* (K. Donaldson and P. Borm, Eds.), Chapter 3. pp. 47–74. CRC Press, Boca Raton, FL.

Kreyling, W. G., Semmler, M., Erbe, F., Mayer, P., Takenaka, S., Shulz, H., Oberdörster, G., and Ziesenis, A. (2002). Translocation of ultrafine insoluble iridium particles from lung epithelium to extrapulmonary organs is size dependent but very low. *J. Toxicol. Environ. Health A* **65,** 1513–1530.

Krieger, M., Semler, M., Erbe, F., Mayer, P., Takenaka, S., Shculz, H., Oberdorster, G., and Ziesenis, A. (2002). Ultrafine insoluble irridium particles are negligibly transported from lung epithelium to extrapulmonary organs.

Kunzli, N., Jerrett, M., Mack, W. J., Beckerman, B., LaBree, L., Gilliland, F., Thomas, D., Peters, J., and Hodis, H. N. (2005). Ambient air pollution and atherosclerosis in Los Angeles. *Environ. Health Perspect.* **113,** 201–206.

Le Brocq, M., Leslie, S. J., Milliken, P., and Megson, I. L. (2008). Endothelial dysfunction: from molecular mechanisms to measurement, clinical implications, and therapeutic opportunities. *Antioxid. Redox Signal.* **10,** 1631–1674.

Li, Z., Hulderman, T., Salmen, R., Chapman, R., Leonard, S. S., Young, S. H., Shvedova, A., Luster, M. I., and Simeonova, P. P. (2007). Cardiovascular effects of pulmonary exposure to single-wall carbon nanotubes. *Environ. Health Perspect.* **115,** 377–382.

Lundqvist, M., Stigler, J., Elia, G., Lynch, I., Cedervall, T., and Dawson, K. A. (2008). Nanoparticle size and surface properties determine the protein corona with possible implications for biological impacts. *Proc. Natl. Acad. Sci. U.S.A.* **105,** 14265–14270.

Meissner, T., Potthoff, A., and Richter, V. (2009). Physico-chemical characterization in the light of toxicological effects. *Inhal. Toxicol.* **2**(Suppl. 1), 35–39.

Mills, N. L., Donaldson, K., Hadoke, P. W., Boon, N. A., MacNee, W., Cassee, F. R., Sandstrom, T., Blomberg, A., and Newby, D. E. (2009). Adverse cardiovascular effects of air pollution. *Nat. Clin. Pract. Cardiovasc. Med.* **6,** 36–44.

Mills, N. L., Tornqvist, H., Gonzalez, M. C., Vink, E., Robinson, S. D., Soderberg, S., Boon, N. A., Donaldson, K., Sandstrom, T., Blomberg, A., *et al.* (2007). Ischemic and thrombotic effects of dilute diesel-exhaust inhalation in men with coronary heart disease. *N. Engl. J. Med.* **357,** 1075–1082.

Mills, N. L., Tornqvist, H., Robinson, S. D., Gonzalez, M., Darnley, K., MacNee, W., Boon, N. A., Donaldson, K., Blomberg, A., Sandstrom, T., *et al.* (2005). Diesel exhaust inhalation causes vascular dysfunction and impaired endogenous fibrinolysis. *Circulation* **112,** 3930–3936.

Mills, N. L., Amin, N., Robinson, S. D., Anand, A., Davies, J., Patel, D., de la Fuente, J. M., Cassee, F. R., Boon, N. A., MacNee, W., Millar, A. M., Donaldson, K., Newby, D. E., *et al*. (2005). Do inhaled carbon nanoparticles translocate directly into the circulation in humans? *Am J Respir. Crit. Care Med.* **173,** 426–431.

Nadziejko, C., Fang, K., Chen, L. C., Cohen, B., Karpatkin, M., and Nadas, A. (2002). Effect of concentrated ambient particulate matter on blood coagulation parameters in rats. *Res. Rep. Health Eff. Inst.* **111,** 7–29.

Nemmar, A., Hoylaerts, M. F., Hoet, P. H., Dinsdale, D., Smith, T., Xu, H., Vermylen, J., and Nemery, B. (2002a). Ultrafine particles affect experimental thrombosis in an in vivo hamster model. *Am. J. Respir. Crit. Care Med.* **166,** 998–1004.

Nemmar, A., Hoylaerts, M. F., Hoet, P. H., and Nemery, B. (2004). Possible mechanisms of the cardiovascular effects of inhaled particles: systemic translocation and prothrombotic effects. *Toxicol. Lett.* **149,** 243–253.

Nemmar, A., Hoylaerts, M. F., Hoet, P. H., Vermylen, J., and Nemery, B. (2003a). Size effect of intratracheally instilled particles on pulmonary inflammation and vascular thrombosis. *Toxicol. Appl. Pharmacol.* **186,** 38–45.

Nemmar, A., Nemery, B., Hoet, P. H., Vermylen, J., and Hoylaerts, M. F. (2003b). Pulmonary inflammation and thrombogenicity caused by diesel particles in hamsters: role of histamine. *Am. J. Respir. Crit. Care Med.* **168,** 1366–1372.

Nemmar, A., Nemery, B., Hoylaerts, M. F., and Vermylen, J. (2002b). Air pollution and thrombosis: an experimental approach. *Pathophysiol. Haemost. Thromb.* **32,** 349–350.

Oberdorster, G., Maynard, A., Donaldson, K., Castranova, V., Fitzpatrick, J., Ausman, K., Carter, J., Karn, B., Kreyling, W., Lai, D., *et al*. (2005). Principles for characterizing the potential human health effects from exposure to nanomaterials: elements of a screening strategy. *Part Fibre Toxicol.* **2,** 8.

Occupational Safety and Health Administration (OSHA). (1991). *Metal and Metalloid Particulate in Workplace Atmospheres* OSHA ID121. OSHA, Sandy City, UT.

Pekkanen, J., Brunner, E. J., Anderson, H. R., Tiittanen, P., and Atkinson, R. W. (2000). Daily concentrations of air pollution and plasma fibrinogen in London. *Occup. Environ. Med.* **57,** 818–822.

Radomski, A., Jurasz, P., onso-Escolano, D., Drews, M., Morandi, M., Malinski, T., and Radomski, M. W. (2005). Nanoparticle-induced platelet aggregation and vascular thrombosis. *Br. J. Pharmacol.* **146,** 882–893.

Renwick, L. C., Donaldson, K., and Clouter, A. (2001). Impairment of alveolar macrophage phagocytosis by ultrafine particles. *Toxicol. Appl. Pharmacol.* **172,** 119–127.

Semmler, M., Seitz, J., Erbe, F., Mayer, P., Heyder, J., Oberdorster, G., and Kreyling, W. G. (2004). Long-term clearance kinetics of inhaled ultrafine insoluble iridium particles from the rat lung, including transient translocation into secondary organs. *Inhal. Toxicol.* **16,** 453–459.

Sun, Q., Wang, A., Jin, X., Natanzon, A., Duquaine, D., Brook, R. D., Aguinaldo, J. G., Fayad, Z. A., Fuster, V., Lippmann, M., *et al*. (2005). Long-term air pollution exposure and acceleration of atherosclerosis and vascular inflammation in an animal model. *JAMA* **294,** 3003–3010.